JOURNAL OF APPLIED ELECTROCHEMISTRY 21 (1991) 885–894

Anodic stability of propylene carbonate electrolytes at potentials above 4 V against lithium: an on-line MS and *in situ* FTIR study‡

E. CATTANEO*, B. RASCH, W. VIELSTICH

Institute of Physical Chemistry, University of Bonn, Wegelerstrasse 12, D-5300 Bonn 1, Germany

Received 25 January 1991; revised 15 March 1991

On-line mass spectroscopy (DEMS) and *in situ* FTIR spectroscopy provide a valuable extension to classical cyclic voltammetry since they enable the identification of reaction products as a function of applied potential. We have compared the CO_2 evolution during the electrooxidation of 0.5 M $LiAsF_6$, 0.5 M $LiBF_4$ and 0.5 M $LiClO_4$/propylene carbonate on platinum combining these techniques. The highest CO_2 formation rate was measured for 0.5 M $LiClO_4$/PC and the lowest for 0.5 M $LiAsF_6$, both with an on-set potential at 4.0 V against Li/Li^+. On-line MS results in 0.5 M $LiBF_4$/PC show strong evidence for the formation (above 4.7 V) of carbonyl fluoride and other fluorinated species parallel to the CO_2 evolution. This indicates an anodic decomposition of BF_4^- anions interacting with oxidized PC species. The role of the OH^- ions on the film formation on platinum at 2.0 V against Li/Li^+ was also investigated with *in situ* FTIR for the three electrolytes.

1. Introduction

The development of rechargeable lithium systems involves the search for solutions to a wide range of problems which include practical questions concerning costs, security and environmental pollution. Some difficulties stem from key properties of the materials employed; they include the high reactivity of lithium metal, availability of rechargeable positive electrodes, corrosion and stable aprotic solvents having adequate Li salts. On the other hand cell components are chosen to fulfill given requirements such as a wide range of operating temperature, high capacity and high energy density. The success of a given system depends on a suitable compromise among these different features.

A central issue concerning lithium secondary systems is the life cycle of the cell which mainly depends on the rechargeability of the lithium electrode, i.e. on minimizing Li losses between cycles. This aspect has been intensively investigated for different solvents and Li supporting electrolytes [1].

A second issue concerns the overcharge stability of an electrolyte/solvent system: above a given potential the electrooxidation of the solvent and/or the decomposition of Li salt sets in, leading to a dangerous overpressure in the cell or to a progressive degradation of the electrolyte from cycle to cycle with reduction of the battery life.

There is a suitable potential value at which to set the upper limit for charging the system which determines the amount of reversible charge of the positive electrode for a given charging current. A simple way of determining this potential for a given electrolyte, without considering any particular positive rechargeable electrode, consists in using platinum or glassy carbon as the working electrode in a potentiostatic system. The electrooxidation shows a more or less pronounced increase of the current above a certain potential measured against a reference electrode. Our present work deals with the problem of overcharge stability.

This paper gives results for the electrooxidation on platinum of propylene carbonate solutions of three lithium salts well known for battery application: $LiClO_4$, $LiBF_4$ and $LiAsF_6$. This study combines the usual cyclic voltammetry with on-line mass spectroscopy and *in situ* FTIR spectroscopy. These two methods allow the identification of reaction products and give quantitative hints about the main reaction mechanisms as a function of applied potential. They permit a more reliable determination of the electrooxidation potentials, avoiding uncertainties inherent to current-potential curves (see, for example, [2]).

On-line MS has already been applied to the study of 0.2 M $LiClO_4$/PC on Pt [3] and FTIR for the electrooxidation of 0.5 M $LiClO_4$/PC on polypyrrole, glassy carbon and platinum [4]. A combination of both methods was recently applied to study the influence of H_2O impurities in the electrooxidation/reduction of 0.5 M $LiClO_4$/PC on platinum [5].

2. Experimental details

2.1. *General*

All measurements were performed at room temperature. Potentials are always referred to Li/Li^+.

* Hoppecke Batterien, D-5790 Brilon 2, FRG.
‡ This paper is dedicated to Professor Dr Fritz Beck on the occasion of his 60th birthday.

0021-891X/91 $03.00 + .12

2.2. *Materials*

Propylene carbonate PC (Burdick and Jackson) was dried over molecular sieves for weeks before use. PC solutions were prepared 0.5 M of $LiClO_4$, $LiAsF_6$ and $LiBF_4$ (Fluka p.a.) in a dry box with Li salts previously dried at 170° C ($LiAsF_6$ and $LiClO_4$) and 120° C ($LiBF_4$). A Karl Fischer titration performed with a Metrohm 684 KF coulometer showed an initial water content of 18 p.p.m. for 0.5 M $LiClO_4$/PC and about 40 p.p.m. for both 0.5 M $LiAsF_6$/PC and 0.5 M $LiBF_4$/PC. The water content, checked after each measurement, was found to be somewhat lower than the initial value in the case of on-line MS measurements and about 100 p.p.m. after FTIR measurements (see below). The FTIR measurements in 0.5 M $LiClO_4$/PC were performed in a solution with an initial water content of 18 and 1000 p.p.m. Karl Fischer results are summarized in Table 1. Measured water contents not included in Table 1 are given in the text and in the figure captions.

2.3. *On-line MS measurements*

The experimental set-up used in this work, based on a QMG 112 quadrupole mass spectrometer (Balzers), is described in [6]. The electrochemical cell is shown in Fig. 1. An important modification was introduced for the present case which avoids the problem of water contamination of the electrolyte during the measurement. In the standard set-up the electrochemical cell is attached to the inlet of a differentially pumped MS system. This system pumps slightly the electrolyte through the working electrode consisting of a porous Pt layer on a PTFE membrane situated at the bottom of the cell (see Fig. 1). Volatile reaction products are analysed as a function of applied potential giving on-line information on the electrochemical processes.

When working with aprotic electrolyte systems, however, water contamination from the outside can only be avoided by sealing the cell and bubbling Ar with a slight internal overpressure. Achieving a perfect seal of the cell is not trivial. Although leaks are somewhat compensated by water vapour being pumped through the MS system, our experience tells that the water content of hygroscopic electrolytes increases steadily with time. This is probably due to the formation of water complexes with the Li salts, which cannot be pumped as volatile species. Another disadvantage is that Karl Fischer checks require reintroducing the cell into a glove box; this is a tedious

Table 1. Water impurities after Karl Fischer titration in p.p.m.

Electrolyte	*Initial*	*MS**	*FTIR**
$LiClO_4$/PC	18, 1000†	16	1000
$LiAsF_6$/PC	40	26	116
$LiBF_4$/PC	40	37	89

* Value after the measurement.
† Water was added for FTIR [5].

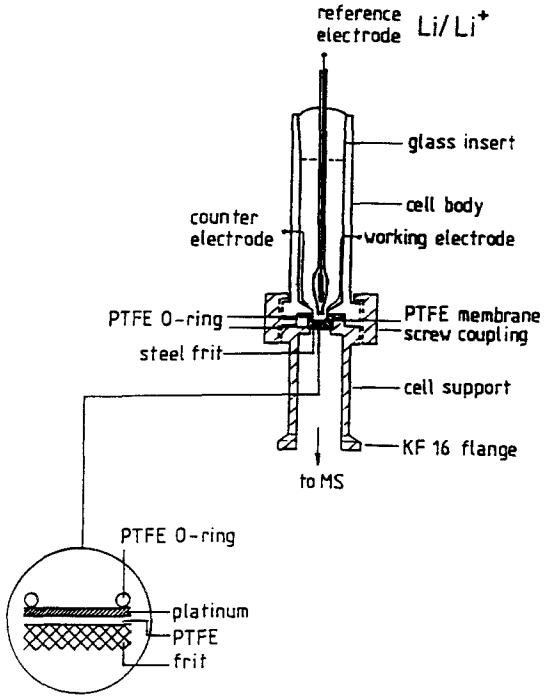

Fig. 1. Electrochemical cell with low electrolyte volume (3 ml) used for on-line mass spectroscopic experiments with porous metal electrodes. The cell body is made out of PTFE.

procedure which endangers the porous Pt electrode (PTFE membrane thickness 75 μm). Water contents obtained this way of less than 100 p.p.m. were an exception.

In a modified set up, the electrochemical cell is placed inside a specially constructed glove box which links the cell outlet with the MS system. This permits the filling and assembling of the cell under a dry argon atmosphere and the bubbling with Ar is no longer necessary. In addition the pumping of the cell from the MS system gives a somewhat lower H_2O content of solutions compared to the initial values (see Table 1).

The cell (Fig. 1) was constructed from PTFE. The reference electrode was a strip of lithium metal dipped into the base electrolyte and separated by a frit from the working electrode compartment. A Pt foil served as counter electrode. The working electrode used for comparing the CO_2 formation of the different Li salt electrolytes was a porous platinum layer with an active surface of 190 cm^2 determined from cyclic voltammograms in 0.5 M H_2SO_4 according to [7]. This large active area renders higher mass signals for the reaction products resulting in a better sensitivity. The current density was calculated using this area. The geometrical area amounts to 0.63 cm^2, so that current densities calculated from it, would give a larger value by a factor of 301. For comparing quantitatively the gas evolution of a same species (e.g. CO_2) in different PC electrolytes, it is better to consider measurements performed on the same electrode in order to avoid systematic discrepancies. Volatile products from the oxidation of 0.5 M $LiBF_4$/PC shown in Figs 4 and 5 were measured on a second porous platinum electrode having an active surface of 553 cm^2. The cell was filled with about 3 ml electrolyte.

The on-line MS measurements were performed by sweeping the potential (Wenking LB75 L potentiostat) between 2.0 and 5.4 V against Li/Li^+ periodically (PRODIS 1/161 function generator). The MS control and the data acquisition were performed by means of a PC. The current together with 10 different *m/e* mass signals were recorded as a function of potential over short time intervals of about 250 ms.

2.4. *In situ FTIR measurements*

A variation of the thin layer FTIR method known as SNIFTIRS (Subtractively Normalized Interfacial Fourier Transform Infrared Spectroscopy) was used [8]. A Digilab FTS40 infrared spectrometer equipped with a liquid nitrogen-cooled MCT detector was employed [9].

A thin layer, one-compartment spectroelectrochemical glass cell provided with a CaF_2 window was used. The working electrode was a 7 mm diameter polycrystalline Pt disc sheathed in Araldite. The i.r.-reflecting Pt electrode was mechanically polished by 0.05 μm alumina powder and then sonicated, first in dilute HNO_3 for 5 min and finally in water for 30 min. As a counter electrode a Pt wire loop was used. The reference electrode was a small strip of freshly scraped lithium, dipped into the electrolyte. The cell was dried, assembled, filled with electrolyte and hermetically sealed in the glove box before fixing into the FTIR instrument. The electrode was pushed against the optical window prior to the measurements.

Before starting the i.r. measurements, for each solution the cell was placed in the sample compartment of the i.r. instrument for 2 h. This time was needed for thermal stabilisation of the electrolyte in the cell allowing a reliable reference spectrum to be obtained.

The potential was then stepped (Stonehart BC1200 potentiostat, PRODIS 1/161 function generator) from 3.6 V down to 2.0 V and further up to 5.0 V. At each potential 256 scans at a 2 cm^{-1} resolution were obtained. These spectra were co-added and averaged to get a single-beam spectrum R. The SNIFTIRS reflectance spectrum was then calculated as R/R_0, where R_0 denotes the reference single beam spectrum.

3. Results and discussion

3.1. *Voltammetry*

Current density against potential curves for 0.5 M $LiClO_4$/PC (a), 0.5 M $LiBF_4$/PC (b) and 0.5 M $LiAsF_6$/PC (c) are given in Fig. 2. These curves show stationary cyclic voltammograms measured at 4 mV s^{-1}. Stability was reached after about 10 cycles. Some irreproducibility, however, remained for $LiBF_4$. All these measurements were performed on the same platinum electrode and the current density was calculated with the real surface (see § 2.3) of the electrode.

An increase of the current density with increasing potential is observed for the three electrolytes above 4 V against Li/Li^+. The current increases at different

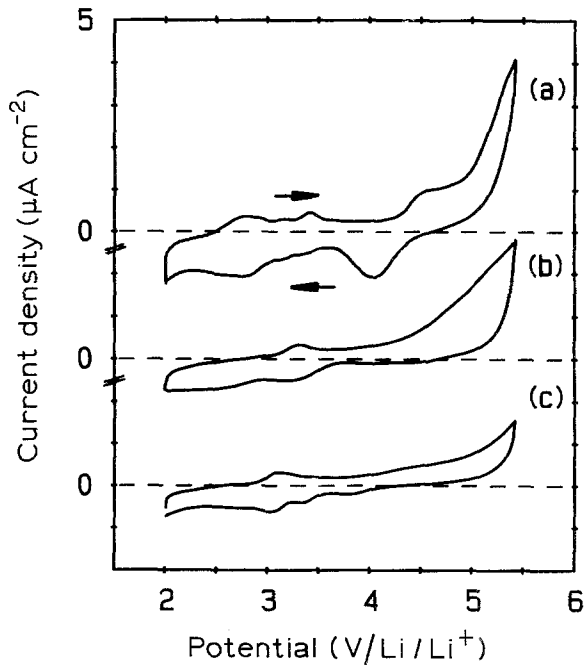

Fig. 2. Stationary cyclic voltammograms (4 mV s^{-1}) in (a) 0.5 M $LiClO_4$/PC, (b) 0.5 M $LiBF_4$/PC and (c) 0.5 M $LiAsF_6$/PC measured on the same platinum porous electrode. The water content of the electrolytes is given in Table 1. The current densities were calculated using the real surface (190 cm^2).

rates: the lowest rate corresponds to $LiAsF_6$ and the highest to $LiClO_4$ which also shows a current plateau at about 4.5 V preceeding a monotonic increase. This steep increase of the current at high anodic potentials in 0.5 M $LiClO_4$/PC suggests a strong PC oxidation confirmed by on-line MS and FTIR as shown below. Similarly the low currents for the other two electrolytes indicate a lower degree of PC degradation. Noteworthy is the minimum on the reverse scans at 4.1 V in 0.5 M $LiClO_4$/PC, which is absent in 0.5 M $LiBF_4$/PC and appears very small and shifted to a lower potential (3.8 V) in 0.5 M $LiAsF_6$/PC.

The current alone, however, gives little information about underlying electrochemical processes (oxidation products are not known), i.e. we have an incomplete picture. For example the current plateau in $LiClO_4$/PC hampers an accurate determination of the on-set potential for the PC oxidation, which is a disadvantage when comparing PC with other solvents (e.g. THF oxidation on platinum in [10]).

One way of overcoming these difficulties, when comparing voltammograms of different systems is to adopt a convention: the oxidation potential is determined by the potential value at which the current density reaches a particular value, for example 100 μA cm^{-2} on glassy carbon [11] or 500 μA cm^{-2} on platinum [12].

An advantage of on-line and *in situ* electrochemical methods, however, is their independence of arbitrary conventions and the additional information they offer for solving the ambiguous cases mentioned.

3.2. *On-line mass spectroscopy*

This technique provides information about different volatile products of the electrooxidation since several

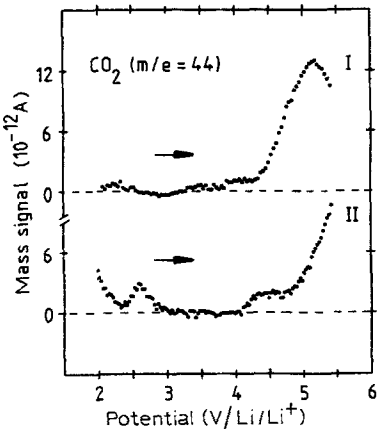

Fig. 3. Mass signals for m/e = 44 as function of potential showing CO_2 formation in (I) 0.5 M $LiBF_4$/PC and (II) 0.5 M $LiAsF_6$/PC on a porous platinum electrode. These curves were measured at 4 mV s^{-1} simultaneously with the anodic scans of the voltammograms shown in Fig. 2.

masses (m/e ratios) can be measured simultaneously during a single cyclic voltammogram.

3.3. *$LiAsF_6$ and $LiBF_4$ solutions*

Figure 3 shows the CO_2 (m/e = 44) mass signal as function of potential for 0.5 M $LiBF_4$/PC (curve I) and 0.5 $LiAsF_6$/PC (curve II), corresponding to the anodic scans of the current density curves in Fig. 2. Curves I and II confirm the electrooxidation of PC above 4.0 V. Some differences are noteworthy: in 0.5 M $LiAsF_6$/PC the CO_2 mass signal goes through a step starting at 4.0 V and increases monotonically above 4.8 V; the current (c in Fig. 2) shows a monotonic increase with a slight change of slope at 4.3 V. In 0.5 M $LiBF_4$/PC a strong CO_2 evolution develops above 4.3 V which correlates with the increase in current density (b in Fig. 2). While the current increases continuously, the CO_2 mass signal (curve I) goes through a maximum at 5.2 V: a hint of some alternative reaction path.

The potential dependence of other mass fragments belonging to volatile products from the 0.5 M $LiBF_4$/PC electrooxidation were investigated by scanning all m/e mass signals between 10 and 100u (atomic mass units) as a function of potential in groups of ten at a time. These measurements were performed between 2.8 and 5.4 V against Li/Li$^+$ at 4 mV s^{-1} on a different Pt electrode (see §2.3). Figure 4 shows the potential dependent mass intensities corresponding to m/e = 44 (CO_2) together with m/e = 47, 66 and 31. These three mass signals together with m/e = 44 and 28 (related mainly to CO_2) are the most intensive ones.

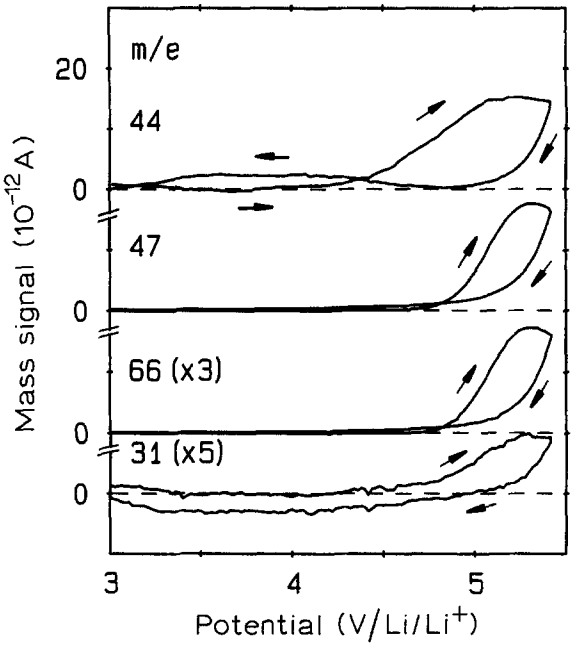

Fig. 4. Mass signals for m/e = 44, 47, 66 and 31 as function of potential (4 mV s^{-1}) in 0.5 M $LiBF_4$/PC (60 p.p.m. H_2O) on a porous platinum electrode (553 cm^2). The potential dependence of the mass fragments 47 and 66 is the same and their intensities are proportional by a factor of 3 suggesting the formation of carbonyl fluoride (COF_2) from the decomposition of BF_4^- anions (see Table 2). These curves were recorded simultaneously.

These mass fragments belong to some (one or more) volatile oxidation product having an on-set potential of 4.7 V (m/e = 47 and 66) and 4.3 V (m/e = 31). Since volatile species with these m/e fragments were not observed in 0.5 M $LiAsF_6$/PC and 0.5 M $LiClO_4$/PC we conclude that they originate from the Li salt i.e. $LiBF_4$. This means that parallel to the electrooxidation of PC a degradation of the salt occurs which leads to the fluorination of oxidation products of PC.

A fragment m/e = 47 may originate in principle from both COF- or C_2H_2F-ions. However, the fact that the potential dependence of the m/e = 66 mass signal is proportional (by a factor of three, see Fig. 4) to m/e = 47 mass signal suggests strongly that they belong to the same substance. This points to carbonyl fluoride COF_2 as best candidate in qualitative agreement with the fragmentation published in the literature (see Table 2).

Only a quantitative discrepancy arises when comparing with literature values. This occurs occasionally when comparing results from different mass spectrometers with different experimental conditions since they affect the fragmentation probabilities. Another source for a quantitative discrepancy may be the

Table 2. Mass spectral data

Compound	*MW**	*m/e*	*fragments (relative abundance)*		
Carb. fluoride [19]	66	47 (100) 12 (3)	66 (55) 50 (2)	28 (14) 16 (1)	31 (4) 48 (1)
2-fluorpropane [20]	62	47 (100)	46 (28)	61 (15)	27 (9)
1,1-difluoroethane [19]	66	51 (100)	65 (50)	47 (9)	15 (4)

* MW: molecular weight.

superposition of mass signals belonging to different species as could be the case of the $m/e = 31$ mass signal (CF-ion) which does not run exactly parallel to the $m/e = 47$ and 66 mass signals (Fig. 4). Evidence for COF_2 formation was briefly reported in [13] for the oxidation of 0.2 M Bu_4NBF_4/PC on platinum.

Potential dependent mass fragments showing increasing mass signals above 4.3 V were also observed for $m/e = 33, 46, 48, 50, 51, 59, 61$ and 65. The largest intensities measured for these fragments are about 40 times smaller than that for $m/e = 47$, being the most intensive the $m/e = 33$ mass signal, corresponding to a CH_2F-ion fragment. Much weaker non reproducible mass signals were observed for $m/e = 35, 63, 64, 69, 77$ and 80, they were not considered in our analysis.

We have investigated different combinations corresponding to probable volatile oxidation products other than COF_2, in particular fluorinated compounds with tertiary linear carbon chains: a good fit for our results is 2-fluorpropane which could explain the potential dependence for the $m/e = 46$ and 61 mass signals shown in Fig. 5. A larger relative intensity between the $m/e = 46$ and the 61 fragment compared to that of the literature (Table 2) and a certain irreproducibility in its value suggest some other contribution from species having a $m/e = 46$ fragment. Unfortunately a quantitative comparison between the $m/e = 47$ and the $m/e = 46$ mass signals is unreliable due to the strong overlapping with the COF-fragment. Evidence for the formation of other tertiary carbon compounds like 2-fluorpropene, allylfluoride and 1-fluorpropane was not found. Fluorinated species like 1,1-difluorethane $C_2H_4F_2$ (see Table 2) could also be formed. An unambiguous identification is however, difficult.

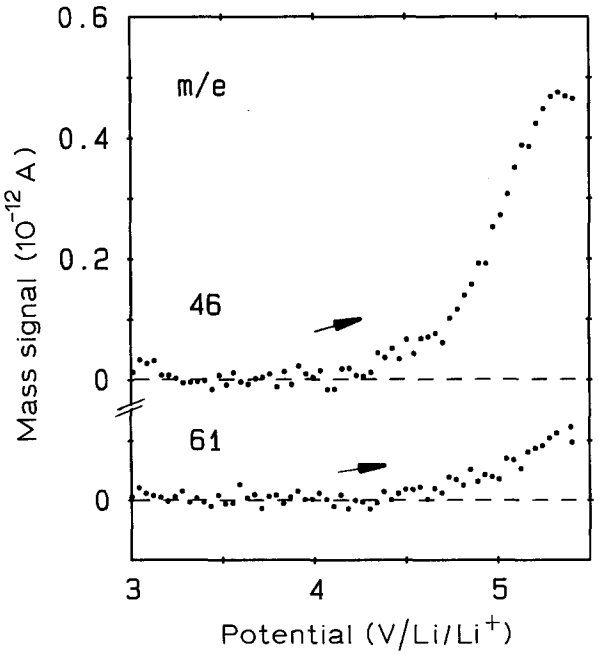

Fig. 5. Mass signals for $m/e = 46$ and 61 as function of potential (anodic scan at 4 mV s^{-1}) in 0.5 M $LiBF_4$/PC (60 p.p.m. H_2O) on the platinum electrode of Fig. 4. The potential dependence of these masses suggests the formation of 2-fluorpropane due to the reaction of BF_4^- ions with oxidized species of PC (see Table 2). The two curves were recorded simultaneously.

As already mentioned, our present analysis is restricted to volatile products. The finding of carbonyl fluoride and other fluorinated species as oxidation products is consistent with the known property of BF_4^- ions to interact with electron deficient organic intermediates in electrochemical oxidation reactions [14]. Through its nucleophilicity BF_4^- acts as a fluorinating agent. In addition other parallel reactions in the electrooxidation of PC leading to ring-opened species occur in $LiAsF_6$/PC and $LiBF_4$/PC. This will be discussed below together with the FTIR results.

3.4. *$LiClO_4$ in PC*

Curve (a) in Fig. 6 shows the CO_2 ($m/e = 44$) mass signal against potential for 0.5 M $LiClO_4$/PC. There are strong qualitative and quantitative differences to 0.5 M $LiBF_4$/PC (Fig. 6, curve b) and 0.5 M $LiAsF_6$/PC (Fig. 6, curve c).

A main difference is the CO_2 maximum at 4.5 V followed by a minimum and a monotonic increase of the CO_2 mass signal. The maximum correlates with the plateau in current density and the subsequent increase of the CO_2 signal correlates with the current increase (Fig. 2, curve a).

No such strong maximum is observed at 4.5 V in the reverse scan shown in curve (a) of Fig. 7. CO_2 formation was mainly observed below 3 V for the $LiClO_4$ (curve a) and $LiAsF_6$ (curve c) electrolytes. The origin of this CO_2 evolution is currently unknown.

In the anodic potential ranges where CO_2 signal and current grow simultaneously there is a linear relationship between both magnitudes. The slopes $\Delta CO_2/\Delta$ current is almost the same for 0.5 M $LiClO_4$/PC and 0.5 M $LiBF_4$/PC and 19% smaller for $LiAsF_6$/PC. This indicates a lower yield of CO_2 per unit of current for the $LiAsF_6$ electrolyte.

If, for 0.5 M $LiClO_4$/PC, we compare the slope $\Delta CO_2/\Delta$ current in the range between 4.2 and 4.6 V with the slope between 5.0 and 5.4 V it is found that the first ratio is about 12 times larger. This remarkable enhancement of the CO_2 production — in the potential region

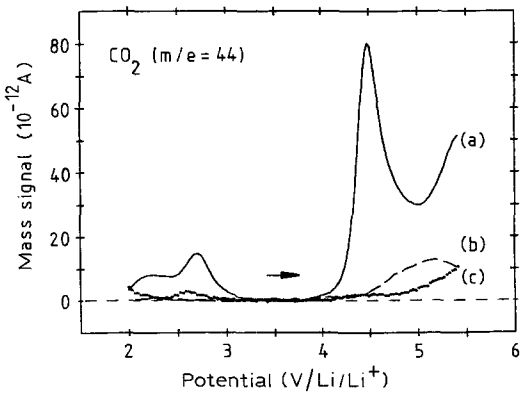

Fig. 6. Mass signals for $m/e = 44$ as function of increasing potential showing CO_2 formation in (a) 0.5 M $LiClO_4$/PC, (b) 0.5 M $LiBF_4$/PC and (c) 0.5 M $LiAsF_6$/PC on a porous platinum electrode (190 cm^2). These curves were recorded at 4 mV s^{-1} simultaneously with the anodic scans of the voltammograms shown in Fig. 2.

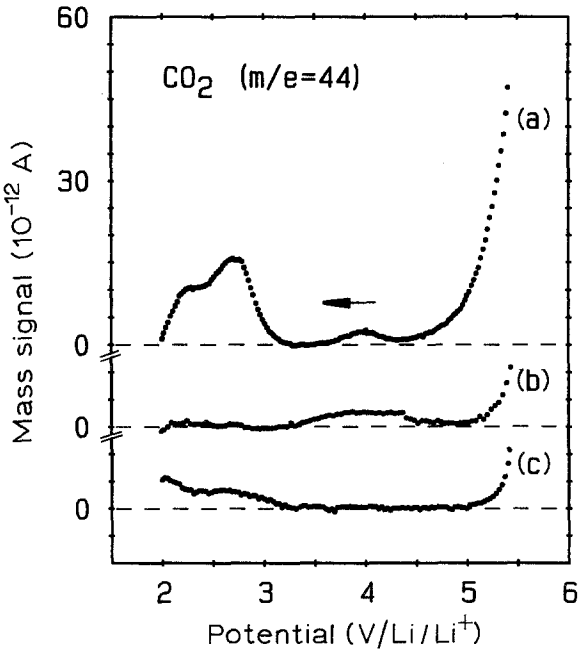

Fig. 7. Mass signals for m/e = 44 as function of decreasing potential showing CO_2 formation in (a) 0.5 M $LiClO_4$/PC, (b) 0.5 M $LiBF_4$/PC and (c) 0.5 M $LiAsF_6$/PC on a porous platinum electrode (190 cm^2). These curves were recorded at 4 mV s^{-1} simultaneously with the cathodic scans of the voltammograms shown in Fig. 2. They correspond to the MS reverse scans of Fig. 6.

where the current shows a plateau – indicates some qualitatively different reaction mechanism. A common ratio for the different electrolytes in a wide potential range would suggest the same process leading to CO_2 formation for all electrolytes.

In a previous publication [5] it was shown that by increasing the water content in PC an overall enhancement of the CO_2 production is obtained. The current plateau was deduced from an interaction of adsorbed water species on platinum. The present results for 0.5 M $LiClO_4$/PC with 16 p.p.m. H_2O (the lowest H_2O content in [5] was 100 p.p.m.), show that the plateau (though not so pronounced) also remains in the case of much lower amount of water impurities. The maximum in the CO_2 mass signal could be related with some species adsorbed or formed on the platinum surface since this strong maximum is not observed in the reverse scan (curve a in Fig. 7). The fact that other electrolytes ($LiAsF_6$ and $LiBF_4$) do not show these plateaux with simultaneous enhancement of the CO_2 production means that the effect is directly related to the presence of ClO_4^- ions. This adds to the remark in [5] that the enhancement of the CO_2 production is a property related to platinum electrodes: the electrooxidation of 1 M $LiClO_4$/PC on carbon electrodes does not show the features shown in Fig. 2 (curve a) and Fig. 6 (curve a), and the FTIR results in [4], on the other hand, show a much lower CO_2 formation for 0.5 M $LiClO_4$/PC on glassy carbon than on platinum. Consistent with this, preliminary MS voltammetric measurements between 2.8 and 4.2 V on MnO_2 rechargeable electrodes in 1 M $LiAsF_6$/PC and 1 M $LiClO_4$/PC show, by contrast with platinum, similar values for the CO_2 evolution.

It is also important to mention that MS anodic scans in 0.5 M $LiClO_4$/PC on platinum show above 4.4 V the evolution of HCl, ClO_2 and other chlorinated species, which indicates the decomposition of ClO_4^- ions. It is at the moment not clear what influence this could have on the CO_2 evolution. The decomposition of ClO_4^- will be treated in a future publication.

The origin of the enhanced CO_2 formation in the $LiClO_4$ electrolyte still remains an open question.

3.5. *In situ FTIR measurements*

Infrared spectroscopy is an alternative approach for investigating the production of small amounts of CO_2 on platinum electrodes. The intensity of the CO_2 stretching absorption band at 2342 cm^{-1} was taken from a series of spectra (experimental range 4000–1000 cm^{-1}) each measured at a different potential. The CO_2 signals obtained for 0.5 M $LiClO_4$/PC (100 p.p.m. H_2O) by stepping the potential from 3.6 V up to 5 V in [5] were by a factor of 10 larger than those for 0.5 M $LiAsF_6$/PC and $LiBF_4$/PC, in agreement with on-line MS results discussed previously (Fig. 6).

In situ FTIR is a suitable method of detecting electrooxidation products without any restriction to volatile species as in on-line MS, provided that they have infrared active vibration modes. In organic systems like PC, however, an unambiguous identification of a substance is sometimes hampered by overlapping intensities of absorption bands of some common functional groups belonging to different species. In our SNIFTIRS spectra positive-going bands indicate a

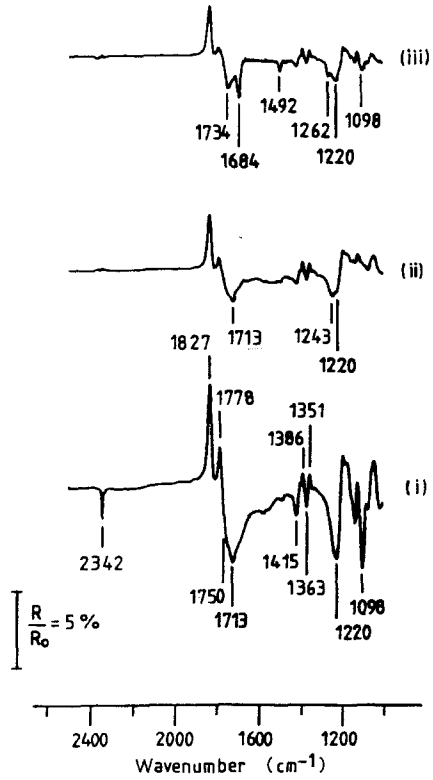

Fig. 8. Sections of FTIR spectra on platinum in (i) 0.5 M $LiClO_4$/PC, (ii) 0.5 M $LiAsF_6$/PC and (iii) 0.5 M $LiBF_4$/PC. The spectra were taken 15 min after setting the potential at 5.00 V against Li/Li^+. The corresponding reference spectra were obtained at 3.60 V (2 cm^{-1} resolution, 256 scans for each spectrum). The water content of the electrolytes is given in Table 1.

decrease in concentration of some species and negative-going bands an increase.

Spectra obtained at 5.0 V against Li/Li^+ for 0.5 M $LiClO_4$/PC + 1000 p.p.m. H_2O, 0.5 M $LiAsF_6$/PC and $LiBF_4$/PC are shown in Fig. 8. The positive going bands at 1827, 1778, 1386 and 1351 cm^{-1} indicate the consumption of PC. The negative-going band in spectrum (i) at 2342 cm^{-1} indicates the CO_2 formation in 0.5 M $LiClO_4$/PC. For the other two electrolytes this band shows a negligible intensity in agreement with the on-line MS results.

The negative-going band at 1098 cm^{-1} in spectrum (i) belongs to ClO_4^- ions [15] migrating into the thin electrolyte layer to compensate charge imbalance due to the formation of electron deficient species (e.g. H^+ ions) during the electrooxidation. No such band is observed in $LiAsF_6$/PC, spectrum (ii), since the AsF_6^- ions adsorb at 700 cm^{-1} [15], a value outside our detection range. The negative-going band at 1098 cm^{-1} in spectrum (iii) corresponds to BF_4^- ions [15]. Other bands appearing in the 1300–1000 cm^{-1} region in spectra (i), (ii) and (iii) belong to ester C–O stretching vibrations [15].

The negative-going bands at 1750 (shoulder), 1415, 1363 and 1220 cm^{-1} are present in all spectra at different potentials for the three electrolytes studied. These bands have intensities stronger than those

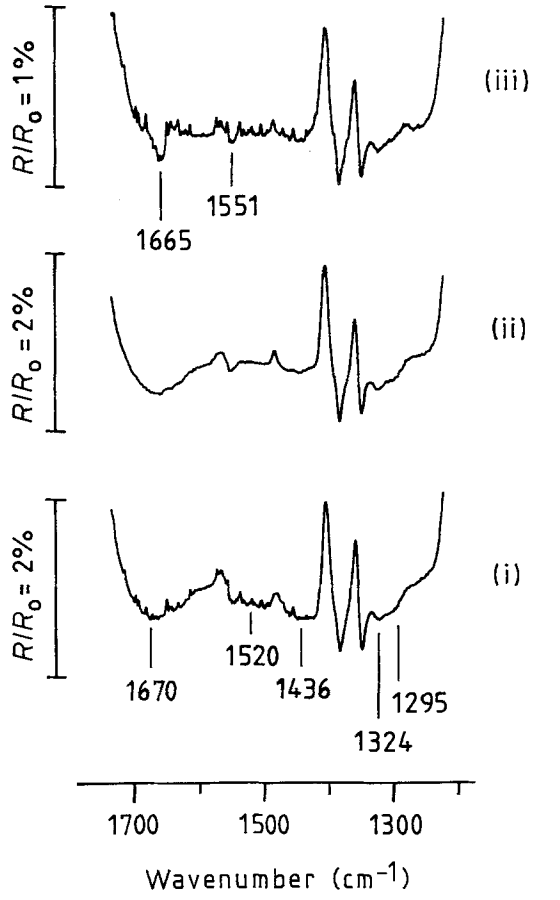

Fig. 9. Sections of FTIR spectra on platinum in (i) 0.5 M $LiClO_4$/PC, (ii) 0.5 M $LiAsF_6$/PC and (iii) 0.5 M $LiBF_4$/PC. The spectra were taken 15 min after setting the potential at 2.00 V against Li/Li^+. The corresponding reference spectra were obtained at 3.60 V (experimental parameters of Fig. 8). The water content of the electrolytes is given in Table 1.

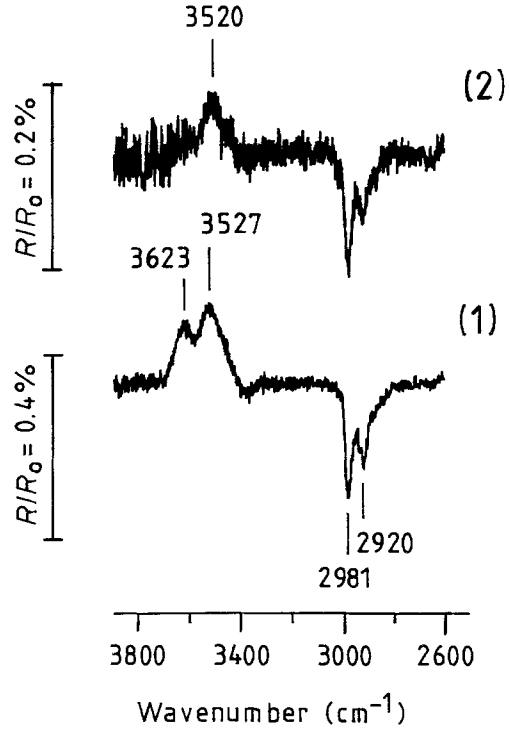

Fig. 10. Sections of FTIR spectra on platinum in (1) 0.5 M $LiAsF_6$/PC and (2) 0.5 M $LiBF_4$/PC belonging to the same spectra with sections (ii) and (iii), respectively, shown in Fig. 9.

expected for adsorbed species [9] and show very small shifts in wavenumbers (about 5 cm^{-1}) to higher values with increasing potential. They appear as positive-going bands when stepping the potential in cathodic direction (e.g. from 3.6 to 2.0 V with the reference spectrum at 3.6 V) so that they cannot be ascribed simply to PC oxidation product(s). We cannot explain at the moment the occurrence of these bands; they are correlated to some PC modes and do not have a counterpart in the region of the C–H stretching vibrations (2981 and 2920 cm^{-1} see Fig. 10 and [5]).

New negative-going bands at 1713 and 1243 cm^{-1} appear during the electrooxidation of the $LiClO_4$ (spectrum (i)) and $LiAsF_6$ (spectrum (ii)) electrolytes above 4.5 V. It is possible to assign these two bands to a (C=O)– (for 1713 cm^{-1}) and (C–O)– (for 1243 cm^{-1}) stretching vibration of some ring-opened species. These bands are observed for example in acetone, propionic acid or higher carbon acids [15]. An unambiguous identification is not a simple task and will require further experiments. Nevertheless we discard the possibility of having propanal due to the fact that no aldehydic absorption band (C–H stretching vibration) was observed at 2720 cm^{-1}, a spectral region where no other bands overlap.

Noteworthy are the differentiated negative-going absorption bands at 1684, 1492 and 1262 cm^{-1} measured for 0.5 M $LiBF_4$/PC (Fig. 8 spectrum (iii)). The 1684 and 1262 cm^{-1} bands seem to belong to the same species having (C=O)– and (C–O)– stretching vibrations as discussed above. The first, however, is shifted to lower and the second to higher energies when compared to the equivalent bands of the $LiClO_4$ and $LiAsF_6$ solutions. These shifted values can be assigned

to carboxylic acids [15]. No satisfactory band assignment was found for the band at 1492 cm^{-1}.

The evaluation of the spectra for 0.5 M $LiBF_4$/PC did not show any characteristic band corresponding to a strong C–F stretching mode which would corroborate the findings of the on-line MS measurements. However, a weak band of 0.04% intensity at 1921 cm^{-1} was observed at 5.4 V. This band can be assigned to the C=O stretching vibration of COF_2 [15].

3.6. *Film formation at 2.0 V against Li/Li$^+$*

In a previous publication [5] we have investigated the film formation on platinum in 0.5 M $LiClO_4$/PC and its dependence on water impurities: a passivation of the electrode at 2.0 V was correlated with a strong CO_2 evolution at 2.6 V in the first scan of MS voltammograms, indicating the subsequent oxidation of the film. In a second scan (following immediately) a much weaker CO_2 mass signal was observed in the same potential ranges; a feature probably due to the oxidation of a much thinner film. This kind of CO_2 formation in the potential region between 2.1 and 3.0 V was also observed for $LiAsF_6$/PC, contrasting with a much weaker CO_2 evolution detected for 0.5 M $LiBF_4$/PC under the same experimental conditions, indicating a much lower rate of film formation for this electrolyte.

The film formation has been investigated for 0.5 M $LiAsF_6$/PC and 0.5 M $LiBF_4$/PC with FTIR using the following procedure: after recording a reference spectrum at 3.6 V the potential was stepped down to 2.0 V. By taking spectra at different times it is possible to detect negative-going bands indicating a film growth. Spectra measured 15 min after setting the potential at 2.0 V are shown in Fig. 9: bands associated with film formation are 1520 and 1436 cm^{-1} corresponding to CO_3^{2-} [16, 17] and 1670, 1436 and 1324–1295 cm^{-1} which may be assigned according to [16] to $CH_3CH(OCO_2^-)CH_2OH$ (alkyl carbonate). These broad bands in spectra (i) and (ii) are hardly observed in 0.5 M $LiBF_4$ (spectrum (iii), plotted with an amplified scale), which correlates with the mentioned weak CO_2 evolution in the MS voltammograms in the region between 2.1 and 3.0 V.

Therefore we conclude that film formation of the kind observed for 0.5 M $LiClO_4$ and $LiAsF_6$/PC is not evident, or occurs at a much lower rate in 0.5 M $LiBF_4$/PC. These results may be explained in the following way.

In agreement with reaction paths proposed by Aurbach *et al.* [16] a scheme leading to simultaneous forming of carbonate and alkyl carbonate films is:

$$H_2O + e^- \longrightarrow \tfrac{1}{2}H_2 + OH^-$$

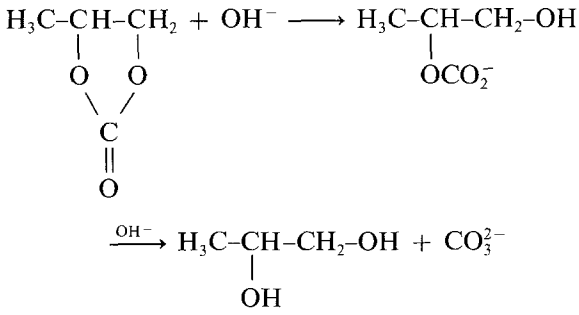

According to this scheme, the film is a consequence of the reaction of PC with strong nucleophilic OH^- ions formed during the water reduction occurring at 2.0 V against Li/Li$^+$. The absence of a film in 0.5 M $LiBF_4$/PC can be readily connected to a small amount of OH^- ions formed in this solution and cannot be derived from the H_2O content, since water impurities are similar (after Karl Fischer) for the $LiBF_4$ and $LiAsF_6$ electrolytes (see Table 1).

Consistent with this, sections of the same FTIR spectra (now in the range 3800–2600 cm^{-1} with a different scale) shown in Fig. 10, provide evidence for a low rate of water reduction in the $LiBF_4$ electrolyte: water consumption is indicated by positive-going bands at 3623 cm^{-1} (antisymmetric stretching) and 3527 cm^{-1} (symmetric stretching) [18] for 0.5 M $LiAsF_6$/PC, in spectrum 1. These bands are much weaker for the $LiBF_4$ electrolyte (spectrum 2, also plotted in an amplified scale).

On-line MS measurements provide indirect evidence for a comparatively low rate of H_2O reduction in 0.5 M $LiBF_4$/PC (60 p.p.m. H_2O): curve (b) in Fig. 11 shows a weaker increase of the H_2 (m/e = 2) formation as function of a cathodic going potential than in 0.5 M $LiAsF_6$/PC (70 p.p.m. H_2O), where a strong H_2 evolution (curve a) sets on below 2.2 V. An inspection of the voltammogram curves measured simultaneously supports these findings (see Fig. 12): The steep decrease in current below 2.1 V in 0.5 M $LiAsF_6$/PC is not observed in 0.5 M $LiBF_4$/PC. A considerable degree of irreproducibility was observed for the $LiBF_4$ electrolyte in the potential region below

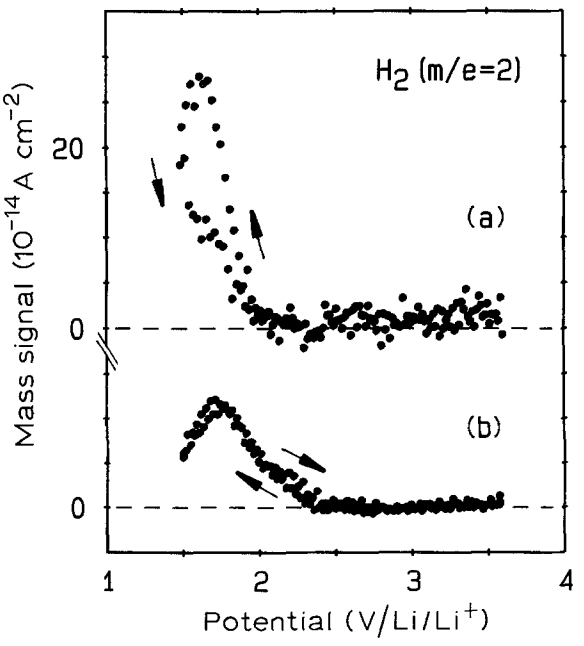

Fig. 11. Mass signal for m/e = 2 as function of potential (4 mV s^{-1}) showing hydrogen formation in (a) $LiAsF_6$/PC (70 p.p.m. H_2O) and (b) $LiBF_4$/PC (60 p.p.m. H_2O) on a porous platinum electrode.

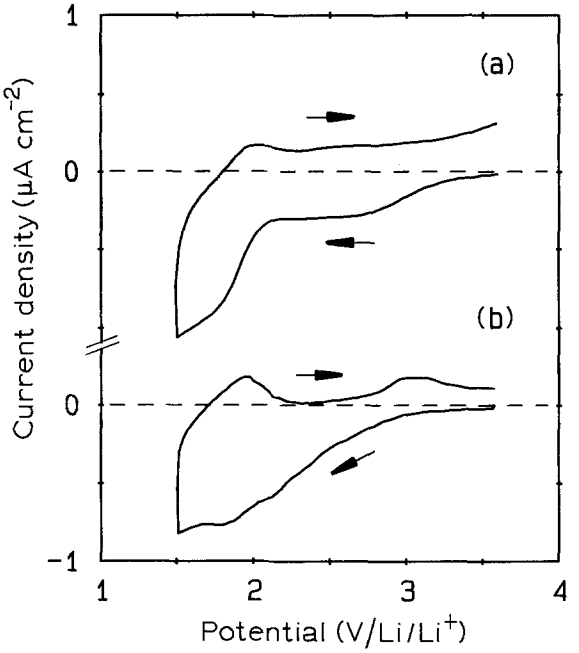

Fig. 12. Current density as function of potential for (a) $LiAsF_6$/PC (70 p.p.m. H_2O) and (b) $LiBF_4$/PC (60 p.p.m. H_2O) on a porous platinum electrode. These voltammograms were recorded simultaneously with the mass signals shown in Fig. 7. The steep increase of the current density below 2.2 V in curve (a) correlates with the on-set of H_2 evolution (see Fig. 11 curve (a)).

2.5 V: occasionally much lower values of hydrogen evolution and current densities were observed than those shown in curve (b) of Fig. 11 and curve (b) of Fig. 12, respectively.

The H_2 evolution for similar experiments in 0.5 M $LiClO_4$/PC (with equivalent amounts of H_2O impurities) were higher by a factor of two than the corresponding for 0.5 M $LiBF_4$/PC.

4. Conclusions

The application of on-line mass spectroscopy and *in situ* infrared spectroscopy to the study of the anodic stability of propylene carbonate solutions with different lithium salts on platinum gives an example for the possibilities of these relatively new techniques as a complement to voltammetry.

Our MS results show that the CO_2 formation sets on for 0.5 M $LiBF_4$/PC, 0.5 M $LiAsF_6$/PC and 0.5 M $LiClO_4$/PC above 4.0 V against Li/Li^+ with different rates, the highest for $LiClO_4$ the lowest for $LiAsF_6$. FTIR measurements corroborate these results on the CO_2 evolution and show also the formation of ring-opened species above 4.5 V for the three PC electrolytes. These oxidized species indicate the existence of alternative reaction paths to those leading to CO_2 formation.

On-line MS results also provide strong evidence for a decomposition of BF_4^- ions in 0.5 M $LiBF_4$/PC, occuring above 4.7 V against Li/Li^+ parallel to the electrooxidation of propylene carbonate. The decomposition of $LiBF_4$ results in the evolution of carbonyl fluoride and other fluorinated species simultaneous with CO_2 formation, indicating a reaction of BF_4^- ions with the electrooxidized species of propylene carbonate.

FTIR measurements at 2.0 V against Li/Li^+ show the formation of carbonate and alkyl carbonate films for $LiAsF_6$ and $LiClO_4$ electrolytes. Such film formation was not evident in 0.5 M $LiBF_4$, a feature that correlates with a lower rate of H_2O reduction in 0.5 M $LiBF_4$/PC compared to that observed in 0.5 M $LiAsF_6$/PC and 0.5 M $LiClO_4$/PC. This suggests that water reduction plays an essential role in this kind of film formation. Our results are in this sense consistent with proposed mechanisms associating alkyl carbonate and carbonate film formation to the reaction of nucleophilic OH^- ions with PC.

The origin of the observed strong CO_2 formation (above 4.0 V) in the $LiClO_4$ electrolyte having only 16 p.p.m. water impurities is still not clear. A current plateau at 4.5 V in 0.5 M $LiClO_4$/PC is associated with a huge CO_2 maximum, several orders of magnitude larger than the corresponding CO_2 production observed for 0.5 M $LiBF_4$ and 0.5 M $LiAsF_6$. Such an enhancement of the oxidation in the $LiClO_4$ electrolyte suggests a different process. The data presented herein together with our previous results indicate that this effect is associated with platinum electrodes and ClO_4^- ions.

Effects of this kind should be taken into account when using platinum electrodes for testing the anodic stability of $LiClO_4$ based electrolytes in battery applications.

Acknowledgements

The authors express appreciation to M. J. Vollmers and H. J. Harms from Hoppecke Batterien for providing the electrolytes. E. C. would like to thank Dr J. Ruch for valuable discussions and suggestions and B. R. acknowledges the Alfried Krupp von Bohlen und Halbach-Stiftung for its financial support. This work was supported by Hoppecke Batterien, D-5790 Brilon 2, FRG.

References

[1] K. M. Abraham, 'An Overview' in 'Rechargeable Lithium Batteries', Vol. 90-5 (edited by S. Subbaro, V. R. Koch, B. B. Owens, and W. H. Smyrl), The Electrochemical Society, Pennington NJ (1990).
[2] F. Ossola, G. Pistoia, R. Seeber and P. Ugo, *Electrochim. Acta* **33** (1988) 47; S. Tobishima and A. Yamaji, *ibid.* **29** (1984) 267.
[3] G. Eggert and J. Heitbaum, *ibid.* **31** (1986) 1443.
[4] P. Novák, P. A. Christensen, T. Iwasita and W. Vielstich, *J. Electroanal. Chem.* **263** (1989) 37.
[5] B. Rasch, E. Cattaneo, P. Novák and W. Vielstich, *Electrochim. Acta*, (1991) in press.
[6] B. Bittins-Cattaneo, E. Cattaneo, P. Königshoven and W. Vielstich in 'Electroanalytical Chemistry', Vol. 17 (edited by Allen J. Bard), Marcel Dekker, New York (1991), chap. 3.
[7] T. Biegler, D. A. J. Rand and R. Woods, *J. Electroanal. Chem.* **29** (1971) 269.
[8] A. Bewick and S. Pons in 'Advances in Infrared and Raman Spectroscopy', Vol. 12 (edited by R. J. H. Clark and R. E. Hester) Heyden, London (1985), p. 1.
[9] T. Iwasita, B. Rasch, E. Cattaneo and W. Vielstich, *Electrochim. Acta* **34** (1989) 1073; B. Rasch and T. Iwasita, *ibid.* **35** (1990) 989.
[10] A. N. Dey and E. J. Rudd, *J. Electrochem. Soc.* **121** (1974) 1294.

[11] C. Nanjundiah, J. L. Goldman, L. A. Dominey and V. R. Koch, *ibid.* **135** (1988) 2914.
[12] S.-I. Tobishima and T. Okada, *Electrochim. Acta* **30, 2** (1985) 1715.
[13] G. Eggert, Dissertation, University Bonn (1986), unpublished.
[14] V. R. Koch, L. L. Miller, D. B. Clark, M. Fleischmann, T. Joslin and D. Fletcher, *J. Electroanal. Chem.* **43** (1973) 318; D. B. Clark, M. Fleischmann and D. Fletcher, *ibid.* **42** (1973) 133.
[15] G. Socrates, 'Infrared Characteristic Group Frequencies', Wiley & Sons, New York (1980).
[16] D. Aurbach and H. Gottlieb, *Electrochim. Acta* **34** (1989) 141.
[17] G. Nazri and R. H. Muller, *J. Electrochem. Soc.* **132** (1985) 2050.
[18] D. Cogley, M. Falk, J. Butler and E. Grunwald, *J. Phys. Chem.* **76** (1972) 855.
[19] Eight Peak Index of Mass Spectra, Vol. 1, Mass Spectrometry Data Centre, Unwin Brothers, GB (1974).
[20] Atlas of Mass Spectral Data, Vol. 1 (edited by E. Stenhagen, S. Abrahamsson and F. W. McLafferty), Wiley & Sons, New York (1969).